

Article

Effect of Asphaltenes and Asphaltene Dispersants on Wax Precipitation and Treatment

Oualid M'barki ¹, John Clements ² and Quoc P. Nguyen ^{1,*}

¹ Hildebrand Department of Petroleum and Geosystems Engineering, The University of Texas at Austin, 200 E. Dean Keeton Stop C0300, Austin, TX 78712, USA; oualid.m'barki@utexas.edu

² Indorama Ventures, 24 Waterway, The Woodlands, TX 77380, USA; john.clements@us.indorama.net

* Correspondence: quoc_p_nguyen@mail.utexas.edu

Abstract: A detailed understanding of the interactions between wax and asphaltenes with other components of crude oils and the effect of treatments with paraffin inhibitors (PIs) and asphaltene dispersants (ADs), with a focus on identifying specific structure-activity relationships, is necessary to develop effective flow assurance strategies. The morphological and rheological consequences of treating wax and asphaltenes in oils of differing composition with a series of ADs having structural features in common with an alpha olefin-maleic anhydride (AO-MA) comb-like copolymer PI were assessed alone and in combination with said PI. Of the four ADs studied, two were identified as being effective dispersants of asphaltenes in heptane-induced instability tests and in a West Texas (WT) crude. The degree to which a low concentration of asphaltenes stabilizes wax in the absence of treatment additives is lessened in oils having greater aromatic fractions. This is because these stabilizing interactions are replaced by more energetically favorable aromatic–asphaltene interactions, increasing oil viscosity. Treatment with AD alone also reduces the extent of wax–asphaltene interactions, increasing oil viscosity. In concert with the PI, treatment with the AD having greater structural similarity with the PI appears to improve wax solubility in both the presence and absence of asphaltenes. However, the viscosity of the treated oils is greater than that of the oil treated with PI alone, while treatment with AD having lesser structural similarity with the PI does not adversely affect oil viscosity. These data suggest that rather than treating both wax and asphaltenes, AD may poison the function of the PI. These data illuminate the pitfalls of designing flow assurance additives to interact with both wax and asphaltenes and developing treatment plans.



Citation: M'barki, O.; Clements, J.; Nguyen, Q.P. Effect of Asphaltenes and Asphaltene Dispersants on Wax Precipitation and Treatment. *Colloids Interfaces* **2024**, *8*, 30. <https://doi.org/10.3390/colloids8030030>

Academic Editor: Plamen Tchoukov

Received: 9 April 2024

Revised: 9 May 2024

Accepted: 10 May 2024

Published: 14 May 2024



Copyright: © 2024 by the authors. Licensee MDPI, Basel, Switzerland. This article is an open access article distributed under the terms and conditions of the Creative Commons Attribution (CC BY) license (<https://creativecommons.org/licenses/by/4.0/>).

1. Introduction

Wax and asphaltenes are stabilized in crude oils by the presence of light hydrocarbons such as methane and ethane as well as by high temperatures and pressures within the formation. When lifted to the surface, these oils are exposed to lower temperatures and pressures and the loss of light ends through evaporation may also occur, destabilizing wax and asphaltic components [1]. Separation and deposition of these components are known to cause significant challenges in oil production and transportation [2–6]. Containing 16 or more carbons, wax consists of linear, branched, and cyclic saturated hydrocarbons having freezing points as high as 90 °C when isolated [7]. In sufficient concentrations, van der Waals (vdW) forces between neighboring wax molecules can overcome the forces associated with solvation such that crystals consisting of wax platelets can form. These precursors can grow to form macroscopic deposits capable of blocking flow lines. Pour point depressants or paraffin inhibitors (PIs) interact with paraffin, interrupting wax crystal growth and preventing the formation of macroscopic deposits. As such, treatment with PIs will often reduce oil viscosity, particularly at lower temperatures, and can also reduce the wax appearance temperature (WAT) depending on how the WAT is defined [3,8–15].

The effects of oil and wax composition on the morphological and rheological consequences of treatment with maleic anhydride-alpha olefin (MA-AO) comb copolymer paraffin inhibitors (PIs, Structure I) have been investigated [16–19]. A series of PIs were selected and their effect on wax was evaluated in a simple wax-containing dodecane-based oil. The PIs were synthesized by the copolymerization of maleic anhydride and alpha-olefin, followed by a reaction of the anhydride in the copolymer with alkyl alcohols to give corresponding alkyl side chains. The molar ratio of alkyl sidechains to maleic units in the PIs, referred to as the sidechain density, ρ_{sc} , was found to be a better predictor of PI performance than the average carbon number of the sidechains. PIs having higher ρ_{sc} values were found to have greater efficacies, i.e., greater reductions in WAT and viscosity of treated oils relative to their untreated counterparts, than those having lower ρ_{sc} values. Synergies between PI and added asphaltenes were also observed such that oils containing both featured lower WATs and viscosities than oils containing either alone [16].

The efficacies of two PIs, differing in their ρ_{sc} values, and their interaction with wax were then evaluated in a diesel-based oil and a light West Texas (WT) crude to assess the effect of increasing oil complexity on PI performance. In the presence of asphaltenes, the efficacy of the PI having the lower ρ_{sc} improved with increasing oil complexity leading to similar PIs performances in more complex oil. Because the anhydrides in the PI backbone that were not reacted with alcohol were subsequently hydrolyzed, the carboxylic acid density of the PI, ρ_{ca} , is inversely proportional to ρ_{sc} (Section 2.1.2). Interactions between wax and PIs have higher ρ_{ca} , and by extension lower ρ_{sc} , are less energetically favorable than those between wax and PIs having lower ρ_{ca} . We postulated that the presence of semi-polar components such as resins and, to a lesser extent aromatics, mitigate this effect. The fact that this trend was not observed in the absence of asphaltenes suggests that asphaltenes are required to facilitate interactions between wax, PI, resins, and aromatics [17].

Treatments with PIs with effective reductions in WAT and/or viscosity are characterized by their ability to transform continuous or semi-continuous wax crystals into discrete spherulites. Rather than crystal shape or size, the degree to which the crystals interacted with one another and the prevalence of bulk oil channels between crystals was found to be the greatest predictor of rheological performance. In studies involving waxes having different average chain lengths, wax composition dictated morphology to a greater extent than the choice of PI. In the absence of asphaltenes, the efficacy of the PI having the higher ρ_{ca} depended more heavily on wax composition than that having the lower ρ_{ca} , suggesting a steric effect. Because this effect was not observed in the presence of asphaltenes, we concluded that asphaltenes enhance electrostatic effects while minimizing steric effects [18].

In many cases, an effective reduction in the WAT and/or viscosity of crude oils involves the treatment of both wax and asphaltenes. Asphaltene dispersants (ADs) improve the solubility of asphaltenes in the crude and reduce agglomeration to maintain a dispersed state, minimizing deposition [20–22]. It is well-known that the presence of asphaltenes often results in high viscosities in general [23]; however, previous authors have shown that their presence can result in reductions in wax deposition from oils possessing a considerable paraffinic component. The magnitude of the reduction depends on whether the asphaltenes exist in dispersed or flocculated forms, with the former offering larger wax-accessible surface areas than the latter [24–29]. The tendency for asphaltenes to adopt a dispersed form strongly depends on concentration, with greater fractions existing in the said form at lower concentrations.

In the last two decades, a wealth of information concerning the molecular and assembled structures of asphaltenes has been gleaned. It has been established that asphaltene molecules have molecular weights in the range 500–1000 Da and are 750 Da on average [30,31]. A large fraction of these molecules possess a single polycyclic aromatic core having an average of seven fused rings in keeping with the so-called island model. A smaller fraction possesses between two and three cores, each composed of between two and three fused rings, connected through aliphatic linkages in keeping with the so-called archipelago model. Nanoaggregates consisting of 4–10 molecules can form at

concentrations below 0.1 wt.%, for which the molecules form a single disordered π stack. Larger clusters having similar aggregation numbers can form at concentrations above about 0.3 wt.%, according to the Yen-Mullins model first proposed in 2010 [30–32].

In the present study, we investigate the morphological and rheological effects of the treatment of wax and asphaltenes in WT crude using asphaltene dispersants (ADs) that have structural features in common with the MA-AO PIs detailed above. Treatments involving the addition of both ADs and a PI are investigated to better understand the contributions from each and their dependence on oil composition.

2. Materials and Methods

2.1. Materials

2.1.1. Wax-Containing Synthetic Oils

Wax containing synthetic oils were prepared from four bases oils: (1) dodecane, (2) 1:1 *w/w* dodecane:toluene, (3) diesel, grade 2, and (4) West Texas (WT) crude. The oils were treated with 500 ppm of the polymeric, i.e., the active component of each AD and/or PI and heated to 75 °C to completely solubilize the wax prior to being characterized by cross-polarized microscopy (CPM) and rheology. Nomenclature and details of the oil samples studied are listed in Table 1. Densities and SARA compositions of the base oils are given in Table 2. In our previous work [17], the rheological behavior of WT crude oil without wax addition showed that the viscosity versus temperature follows the Arrhenius law up to 1 Celsius, suggesting the absence of wax that could crystallize. A 55/45 *w/w* mixture of two commercial waxes, obtained from Sigma-Aldrich and having melting points of 53–58 °C and 65+ °C [16], was added to the base oils to give synthetic oils containing 10 wt.% wax. This wax content was chosen based on our previous works [16–18] and the fact that various crude oils present in the world contain wax contents between 3 and 40% [33]. The average carbon number of the wax blend is 29.1 ± 3.8 and its number distribution is provided in the Supporting Information. Despite the poor solubility of asphaltenes in hydrocarbons in general, no separation of the asphaltene dispersion was observed in any of the oils over the timescale of the experiments. Furthermore, the rheological characterization of independently prepared samples was found to be quite reproducible.

Table 1. Nomenclature, base oil, wax, and asphaltenes content and AD and PI added for oils studied.

| Oil ¹ | Base Oil | Wax (wt.%) | Asphaltenes (wt.%) | AD ² | PI ² |
|-------------------------|-----------------------|---------------|-----------------------|-----------------|-----------------|
| D _w | Dodecane | 10 | --- | --- | --- |
| D _w -1A | Dodecane | 10 | 1 | --- | --- |
| D _{T,w} | 1:1 Dodecane: Toluene | 10 | --- | --- | --- |
| D _{T,w} -1A | 1:1 Dodecane: Toluene | 10 | 1 | --- | --- |
| D _{L,w} | Diesel | 10 | --- | --- | --- |
| D _{L,w} -1A | Diesel | 10 | 1 | --- | --- |
| WT | WT Crude | --- | --- | --- | --- |
| WT-1A | WT Crude | --- | 1 | --- | --- |
| WT-1A-AD3 | WT Crude | --- | 1 | AD3 | --- |
| WT-1A-AD4 | WT Crude | --- | 1 | AD4 | --- |
| WT _w | WT Crude | 10 | --- | --- | --- |
| WT _w -1A | WT Crude | 10 | 1 | --- | --- |
| WT _w -3A | WT Crude | 10 | 3 | --- | --- |
| WT _w -AD3 | WT Crude | 10 | --- | AD3 | --- |
| WT _w -AD4 | WT Crude | 10 | --- | AD4 | --- |
| WT _w -1A-AD3 | WT Crude | 10 | 1 | AD3 | --- |
| WT _w -1A-AD4 | WT Crude | 10 | 1 | AD4 | --- |
| WT _w -PI | WT Crude | 10 | --- | --- | PI |
| WT _w -AD3-PI | WT Crude | 10 | --- | AD3 | PI |

Table 1. Cont.

| Oil ¹ | Base Oil | Wax (wt.%) | Asphaltenes (wt.%) | AD ² | PI ² |
|----------------------------|----------|---------------|-----------------------|-----------------|-----------------|
| WT _w -AD4-PI | WT Crude | 10 | --- | AD4 | PI |
| WT _w -1A-PI | WT Crude | 10 | 1 | --- | PI |
| WT _w -1A-AD3-PI | WT Crude | 10 | 1 | AD3 | PI |
| WT _w -1A-AD4-PI | WT Crude | 10 | 1 | AD4 | PI |

¹ D = dodecane, DT = 1:1 w/w dodecane:toluene, DL = diesel, WT = West Texas crude. Names that include the subscript 'w' refer to oils containing 10 wt.% added wax. ² AD and PI were added to give concentrations of 500 ppm of the polymeric component of each.

Table 2. Density and SARA analysis of base oils studied.

| | Density ¹ | SARA ² (%) | | | | R/As | CII ³ |
|----------------------|----------------------|-----------------------|------|------|------|------|------------------|
| | | S | Ar | R | As | | |
| Asphaltic crude | 948 | 24.6 | 42.8 | 16.3 | 16.2 | 1.0 | --- |
| Dodecane | | 100.0 | 0.0 | 0.0 | 0.0 | 1.0 | --- |
| D _w | | 100.0 | 0.0 | 0.0 | 0.0 | 1.0 | --- |
| D _w -1A | | 95.8 | 2.4 | 0.9 | 0.9 | 1.0 | 29.5 |
| 1:1 Dodecane:toluene | | 50.0 | 50.0 | 0.0 | 0.0 | --- | 1.0 |
| DT _w | | 55.0 | 45.0 | 0.0 | 0.0 | --- | 1.2 |
| DT _w -1A | | 53.6 | 44.6 | 0.9 | 0.9 | 1.0 | 1.2 |
| Diesel | | 60.0 | 40.0 | 0.0 | 0.0 | --- | 3.0 |
| DL _w | | 64.0 | 36.0 | 0.0 | 0.0 | --- | 3.4 |
| DL _w -1A | | 62.0 | 36.2 | 0.9 | 0.9 | 1.0 | 3.1 |
| WT crude | 849 | 61.7 | 27.5 | 10.8 | 0.0 | --- | 1.6 |
| WT _w | | 65.5 | 24.8 | 9.7 | 0.0 | --- | 1.9 |
| WT _w -1A | | 63.4 | 25.6 | 10.0 | 0.9 | 11.1 | 1.8 |
| WT _w -3A | | 59.3 | 27.3 | 10.6 | 2.7 | 3.9 | 1.6 |

¹ 20 °C, Kg/m³. ² S = saturates, Ar = aromatics, R = resins, and As = asphaltenes. ³ CII = colloidal instability index.

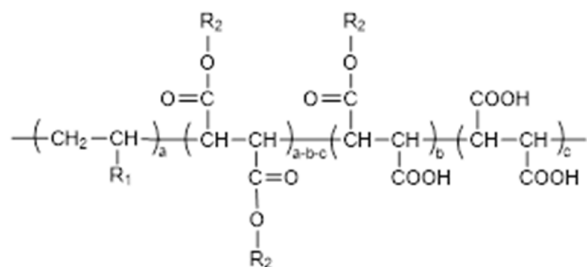
2.1.2. Asphaltenes

The asphaltic crude was found to have an acid value of 0.75 mg KOH/g according to an adaption of the ASTM method D4739 for the determination of base number by potentiometric titration. Asphaltene was isolated from the crude according to ASTM method D6560 and analyzed by GPC. Whereas, the crude is characterized by number-, <Mn>, and weight-, <Mw>, yielding average molecular weights of 560 and 1915 Da, respectively, with a peak molecular weight of 770 Da; the isolated asphaltene in toluene is much heavier, having <Mn>, <Mw>, and peak molecular weights of 2240, 15,360, and 4870 Da, respectively. However, we recognize that intermolecular interactions between asphaltene molecules are generally not disrupted by this form of analysis such that the molecular weights observed are of nanoaggregates and clusters rather than individual molecules. An overlay of the chromatograms is given in the Supporting Information. Elemental analysis via combustion of isolated asphaltenes revealed 83.92 wt.% carbon, 7.92 wt.% hydrogen, 2.06 wt.% oxygen, 1.25 wt.% nitrogen, and 4.21 wt.% sulfur.

2.1.3. Paraffin Inhibitor (PI)

SURFONIC® OFP 961, a commercially available PI provided by Indorama Ventures Oxides & Derivatives LLC, was selected for these studies because its interactions with wax and asphaltenes have been well-documented [16]. The PI consists of an AO-MA alternating copolymer backbone possessing saturated hydrocarbon sidechains and a weight-average molecular weight of ~5000 Da (GPC, THF, 1 mL/min, and poly(propylene glycol) standards). Linear alkyl sidechains, consisting of 21.1 ± 2.2 carbons, are attached via the

reaction of the anhydride in the AO-MA copolymer with mixtures of fatty alcohols to give ester linkages (Scheme 1), with $\rho_{sc} = ((2a - b - 2c))/a = 1.6$ and $\rho_{ca} = ((b + 2c))/a = 0.4$. The distribution of hydrocarbon chains attached via the above-mentioned linkages as well as those originating from the alpha olefin monomers themselves are 21.1 ± 2.2 carbons in length and vary from 16 to 26.



Scheme 1. General structures of AO-MA-derived PIs featuring R1 and R2 hydrocarbon sidechains. Inhibitors possessing linkage attachment of R2 alkyl chains to maleic repeating units are shown.

2.1.4. Asphaltene Dispersants (ADs)

Four asphaltene dispersants, *AD1-AD4*, were also provided by Indorama Ventures Oxides & Derivatives LLC. Each dispersant consists of the reaction product of poly(maleic anhydride) with two or more fatty amines. These products are comb polymers featuring side chains with imide-functional points of attachment (Structure II). With regard to the side-chains, each possesses the same molar ratio of side-chain imide to anhydride moieties with the latter having been subsequently hydrolyzed (Structure II, $a/b = \text{constant} = 0.65$). In each, poly(maleic anhydride) was reacted with two or more of the following five classes of fatty amines: (1) 1-(2-aminoethyl)-2-alkylimidazoline (AEAI), (2) aminated nonylphenol propoxylate (ANPP), (3) aminated C12-14 linear alcohol propoxylate (ALAP), (4) tallowamine (TA), and (5) C16 and C18 Guerbet amine (G16 and G20). The active or polymeric component of each dispersant was solubilized in mixtures of organic solvents such as linear alkylbenzenes, xylene, and toluene. Further structural details can be found in Table 3.

Table 3. Asphaltene dispersant composition and property.

| AD | R | % AEAI ¹ | Pendant Length ² | Active ³ (wt.%) |
|------------|---------------------|---------------------|-----------------------------|----------------------------|
| <i>AD1</i> | AEAI, ANPP, ALAP | 30 | 25.3 | 37 |
| <i>AD2</i> | AEAI, G20 | 52 | 16.9 | 50 |
| <i>AD3</i> | AEAI, TA | 54 | 19.2 | 50 |
| <i>AD4</i> | AEAI, G16 | 38 | 15.0 | 50 |

¹ Molar % of side chains that are AEAI -functional. ² Average equivalent carbon chain length. ³ Polymeric components of the formulation.

2.2. Methods

2.2.1. CPM and Rheological Methods

The methods employed to obtain CPM images and cooling–heating viscosity profiles of the oils have been described elsewhere [16,17]. Viscosity profiles have been used to evaluate the WAT of the waxy oil solution. WAT values for each sample were obtained from their viscosity curves as the on-set temperature at which the rate of viscosity increases becomes more dramatic with further cooling [16,17]. Both methods are, in general, good indicators to evaluate the effect of asphaltenes and asphaltenes dispersants on wax precipitation and treatment as the crystal structure can be directly observed with CPM; rheometry provides

more information about the viscosity of the oil above and below WAT, which is important for understanding and solving wax-related flow assurance issues. However, these methods should be supported by cold finger or flow loop experiments to evaluate wax deposition as presented in our previous study [19].

2.2.2. Asphaltene Precipitation from Toluene

An asphaltic solution in toluene was prepared by mixing an asphaltic crude containing 16 wt.% asphaltenes (Table 2), i.e., heptane insolubles, with toluene in a 1:1 *w/w* ratio using an ultrasonic homogenizer. Treated solutions contained 500 ppm of the polymeric components of AD1-AD4 and PI separately. Heptane-induced instability tests were carried out by adding heptane to obtain a 1:1:40 *w/w/w* ratio of asphaltic crude, toluene, and heptane, respectively. Test solutions were mixed and allowed to stand at 20 °C. CPM images of the solutions were acquired 2 days and 10 days after preparation.

3. Results and Discussion

Maximum viscosity, μ_{\max} , % reduction in μ_{\max} relative to untreated oils, μ_{red} , and WAT obtained by rheological measurements of the oils appearing in Table 1 are summarized in Table 4.

Table 4. μ_{\max} , μ_{red} , and WAT from the cooling–heating viscosity profiles of oils studied.

| Oil | μ_{\max} (cP) | μ_{red} (%) | WAT ¹ (°C) | Shape |
|----------------------------|----------------------|---------------------------|--------------------------|---------|
| D _w | 331 | --- | 35 | Sharp |
| D _w -1A | 91 | 72.5 ² | 23 | Gradual |
| DL _w | 445 | --- | 36 | Sharp |
| DL _w -1A | 374 | 16.0 ³ | 35 | Sharp |
| DT _w | 96 | 72.0 ² | 30 | Medium |
| DT _w -1A | 246 | -156.3 ⁴ | 29 | Medium |
| WT _w | 991 | --- | 38 | Sharp |
| WT _w -1A | 1010 | -1.9 ⁵ | 37 | Sharp |
| WT _w -3A | 3133 | -216.1 ⁵ | 37 | Sharp |
| WT _w -AD3 | 1111 | -12.1 ⁵ | 39 | Sharp |
| WT _w -AD4 | 855 | 13.7 ⁵ | 38 | Sharp |
| WT _w -1A-AD3 | 1382 | -36.8 ⁶ | 38 | Sharp |
| WT _w -1A-AD4 | 1616 | -60.0 ⁶ | 38 | Sharp |
| WT _w -PI | 327 | 67.0 ⁵ | 37 | Medium |
| WT _w -AD3-PI | 367 | 63.1 ⁵ | 37 | Medium |
| WT _w -AD4-PI | 595 | 40.0 ⁵ | 37 | Medium |
| WT _w -1A-PI | 37 | 96.3 ⁵ | --- | --- |
| WT _w -1A-AD3-PI | 33 | 10.8 ⁵ | --- | --- |
| WT _w -1A-AD4-PI | 133 | 259.5 ⁷ | --- | --- |

¹ Onset temperatures. Transitions are characterized as being sharp, medium, or gradual. % reduction in maximum viscosity relative to oil. ² D_w. ³ DL_w. ⁴ DT_w. ⁵ WT_w. ⁶ WT_w-1A. ⁷ WT_w-1A-PI.

3.1. Treatment of Asphaltenes

3.1.1. Heptane-Induced Instability Tests

Solutions of 1:1:40 *w/w/w* asphaltic crude:toluene:heptane were treated with 500 ppm of the separate polymeric components of dispersants AD1-AD4. CPM images of the mixtures, taken after 2 and 10 days, are shown in Figure 1. In all cases, no visible precipitation was observed throughout the duration of the test. However, two days after the addition of heptane, asphaltene deposits were observed by CPM in all cases. Relative to the control, those samples treated with AD feature reductions in both the quantity and size of asphaltene deposits at both two and 10-day intervals. Of the ADs evaluated, samples treated with AD3 and AD4 appear to show the least deposition, particularly after 10 days, with less agglomeration and smaller particles being observed relative to those oils treated with AD1 and AD2.

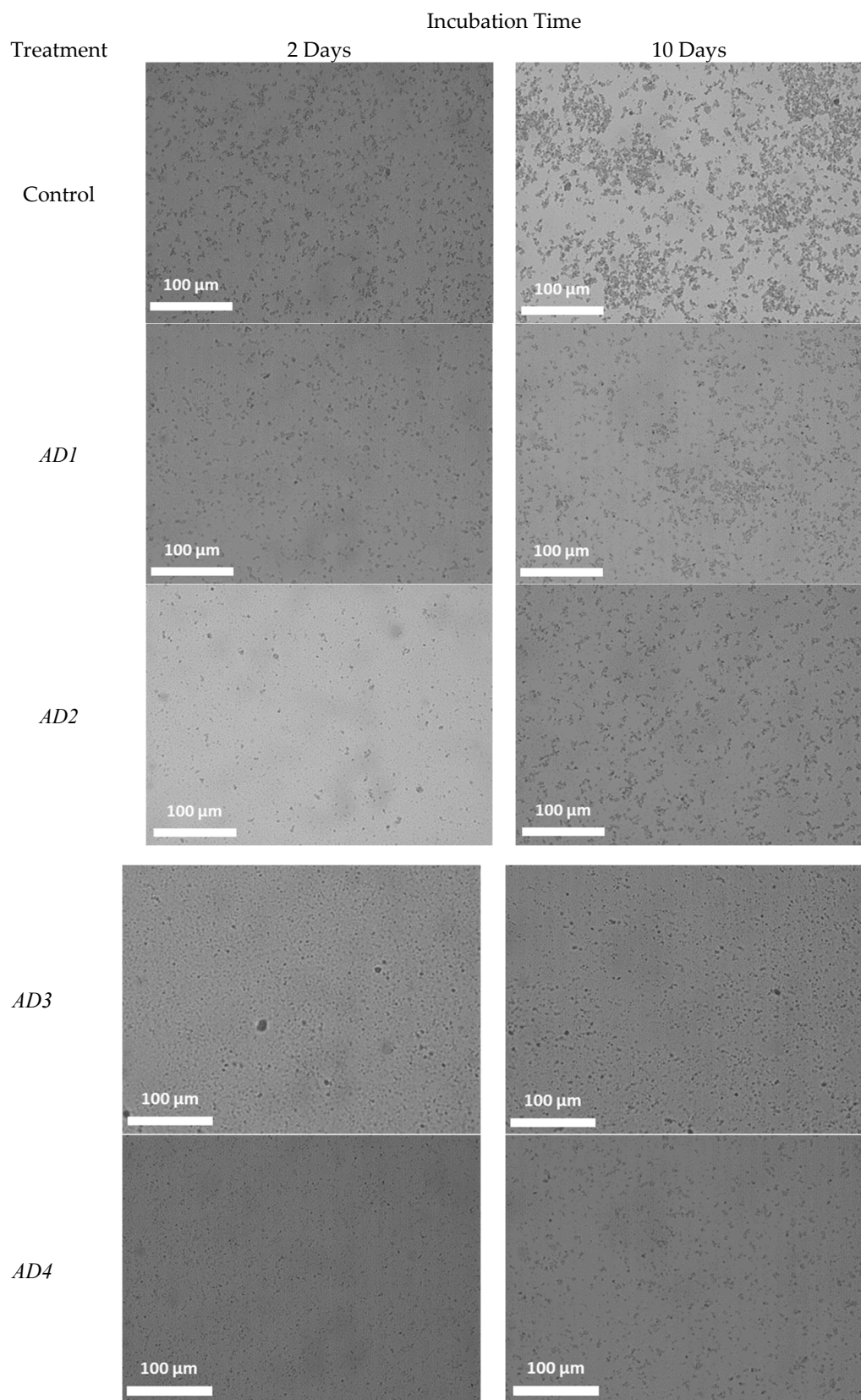


Figure 1. CPM images of simple asphaltene-containing mixtures.

The superior performance of AD3 and AD4 over that of AD1 and AD2 does not correlate with the fraction of sidechains that are imidazoline functional or the average effective sidechain carbon length. Rather, it appears that the propoxylated sidechains in

AD1 do not associate favorably with this asphaltene. *AD2* and *AD4* are the most similar of the dispersants studied, differing only in the length of their Guerbet sidechains. The latter, possessing C20 Guerbet sidechains, performs notably better than the former, possessing the shorter C16 Guerbet sidechains, which is somewhat surprising. Although similar in their performance, it could be argued that *AD3*, possessing C18 tallow sidechains, performs somewhat better than *AD4*.

3.1.2. In WT Crude

Dispersants *AD3* and *AD4*, which performed best in heptane-induced instability tests, were selected for further study in WT crude. Samples of WT crude, oil WT, containing 1 wt.% asphaltenes via addition of asphaltic crude, oil WT-1A, and crudes containing asphaltenes that have been treated with 500 ppm of the polymeric components of *AD3* and *AD4* separately, and oils WT-1A-AD3 and WT-1A-AD4 were prepared. Following equilibration at 20 °C, CPM images of the crudes were obtained and are shown in Figure 2. No deposits were observed in oil WT, not containing added asphaltenes. Asphaltene-containing oils treated with *AD3* and *AD4* exhibit smaller more solvated deposits than those in the untreated oil WT-1A. These findings are similar to those obtained from heptane-induced instability tests, with differences in the images being more readily apparent. Viscosity profiles for the oils are not shown as the maximum viscosity, realized on cooling to ~9 °C, which is only ~10 cP for each, not containing the added wax. These data demonstrate the effectiveness of the dispersants in this crude.

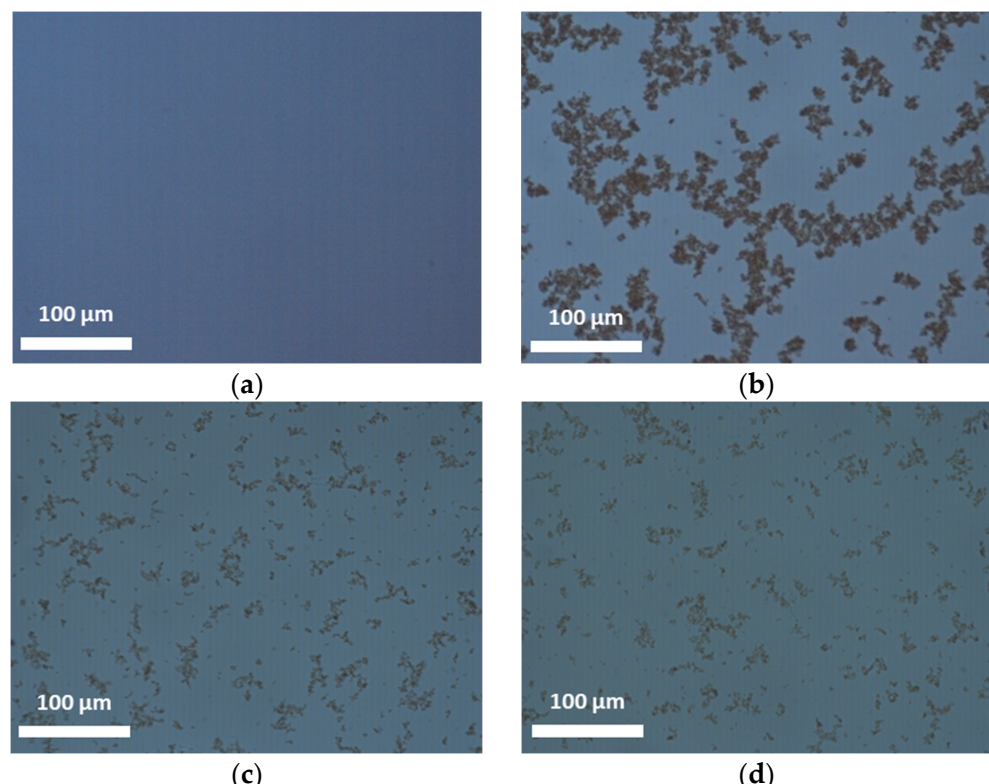


Figure 2. CPM images, taken following equilibration at 20 °C, of oils (a) WT, (b) WT-1A, (c) WT-1A-AD3, and (d) WT-1A-AD4, not containing added wax.

3.2. Effects of Wax and Asphaltenes on the Rheology of Simple Oils and WT Crude

3.2.1. In Simple Oils

The rheometric effects of adding asphaltenes to dodecane, oil D_W, a 1:1 *w/w* blend of dodecane and toluene, oil DT_W, and diesel, DL_W, each containing 10 wt.% added wax, were investigated, with the viscosity cooling–heating profiles of the oils appearing in Figure 3. The addition of asphaltenes to oil D_W reduces the WAT from 35 to 23 °C and renders the

transition more gradual. The maximum viscosity, μ_{\max} , realized on cooling to ~ 9 °C, is also reduced from 331 to 91 cP, i.e., a 72.5% reduction (Figure 3a, Table 4). The CPM images of the oils D_w and D_w -1A are consistent with these observations (see Supporting Information), for which the addition of asphaltenes transforms the needle-like wax crystal network seen in oil D_w to a more amorphous better-solvated network of wax and asphaltenes in oil D_w -1A [16]. In contrast, the addition of asphaltenes to oil DT_w reduces the WAT by only 1°, from 30 to 29 °C, with the shape of the transition being little changed. μ_{\max} is increased from 96 to 246 cP, a 156% increase (Figure 3b). Whereas added asphaltenes interact with and solvate wax in dodecane, they prefer to interact with the large toluene component in oil DT_w , leaving the wax component poorly solvated. The poorly solvated wax, due to the toluene presence, leads to wax crystallization, which increases viscosity. Because the aromatic fraction in diesel-based oil DL_w is only about half that in DT_w , the effects of adding asphaltenes in diesel more closely match those observed in dodecane alone rather than in the dodecane and toluene mixture. The WAT is decreased by only 1°, from 36 to 35 °C, with the shape of the transition remaining sharp, and μ_{\max} is decreased from 445 to 374 cP, a 16% reduction (Figure 3c).

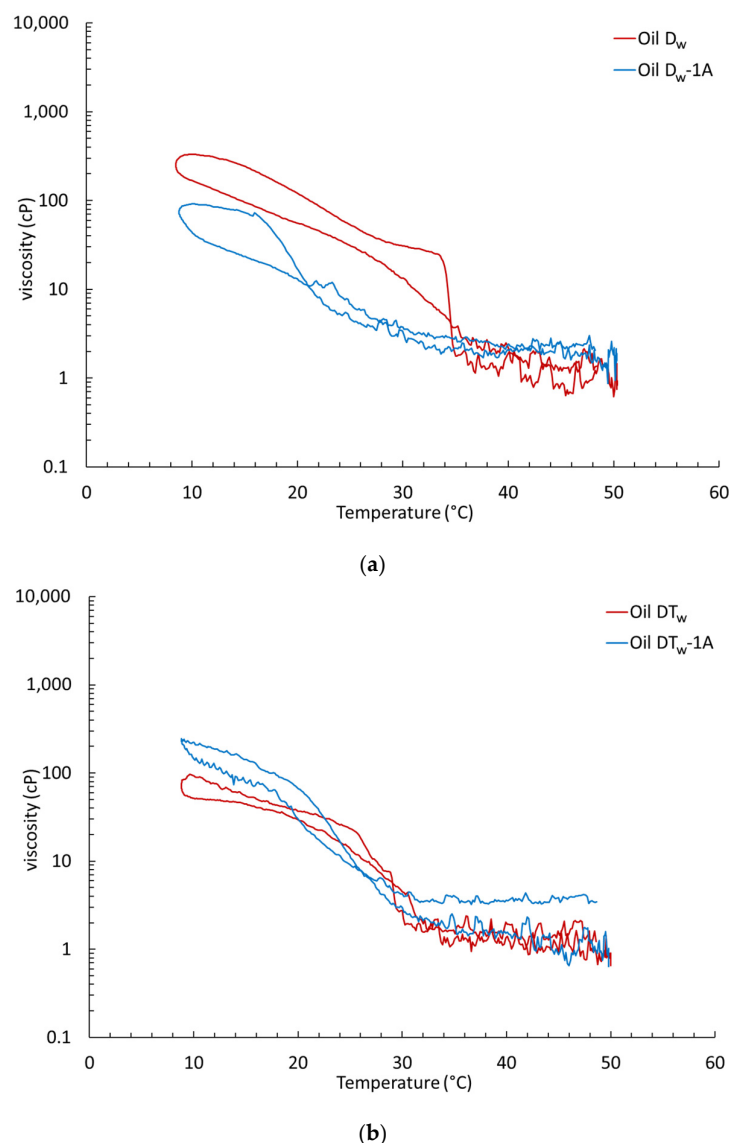


Figure 3. Cont.

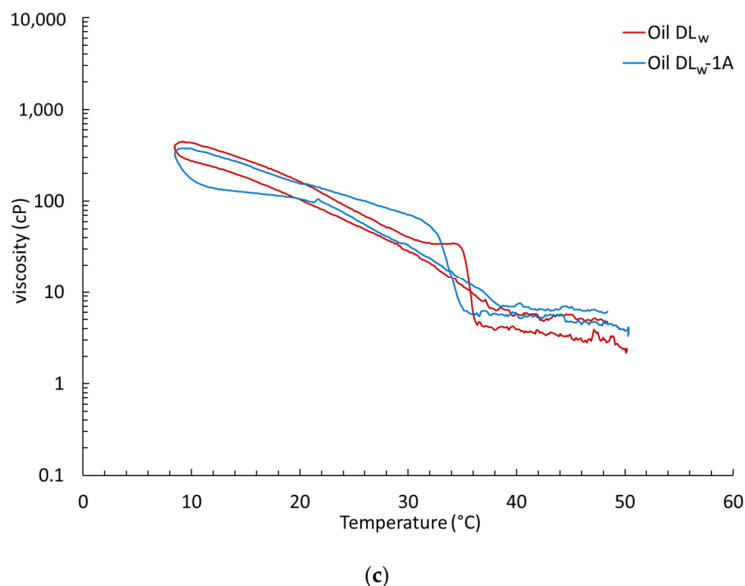


Figure 3. The $50\text{ }^{\circ}\text{C} \rightarrow 8\text{ }^{\circ}\text{C} \rightarrow 50\text{ }^{\circ}\text{C}$ cooling–heating viscosity profiles (cP) for oils (a) D_w (red) and $\text{D}_w\text{-}1\text{A}$ (blue), (b) DT_w (red) and $\text{DT}_w\text{-}1\text{A}$ (blue), and (c) DL_w (red) and $\text{DL}_w\text{-}1\text{A}$ (blue).

It is well known that the presence of resins has a stabilizing effect on asphaltenes. As their geological precursors, resins are thought to act as solvation shells for asphaltenes in crude oils [34]. Indeed, it has been shown that asphaltene clusters consist of ~15% resins [30]. The ratio of resins to asphaltenes, R/As , is often a predictor of oil stability, for which crudes having a R/As ratio less than ~3 tend to exhibit asphaltene precipitation and sedimentation [35]. However, the R/A ratios are 1.0 for each of the oils D_w , DT_w , and DL_w such that the effect of differing ratios is not a factor in this series. Another ratio that is often used to predict oil stability is the colloidal instability index (CII), defined as the ratio of the sum of saturates and asphaltenes to the sum of aromatics and resins, $((\text{S} + \text{As})) / ((\text{Ar} + \text{R}))$ [36]. Oils having lower CII values are more stable, i.e., less likely to phase separately. Generally, asphaltenes and saturates in oils having CII values greater than ~0.9 tend to be poorly solvated, resulting in deposition [34,37,38]. The CII of oil $\text{D}_w\text{-}1\text{A}$, for which the addition of asphaltenes lowers viscosity, is 29.5 and the CII of oil $\text{DT}_w\text{-}1\text{A}$, for which the addition of asphaltenes raises viscosity, is only 1.2, which belies this trend (Table 2). However, these simple oils do not accurately reflect the more complex crudes for which the trend was initially identified. While the saturates component in oil $\text{D}_w\text{-}1\text{A}$ is large, it consists entirely of species that are liquids at room temperature, with only the added wax contributing to oil instability.

3.2.2. In WT Crude

The $50\text{ }^{\circ}\text{C} \rightarrow 8\text{ }^{\circ}\text{C} \rightarrow 50\text{ }^{\circ}\text{C}$ cooling–heating viscosity profiles of WT crude containing 10 wt.% wax, oil WT_w , and 1 and 3 wt.% asphaltenes via the addition of asphaltic crude and the oils $\text{WT}_w\text{-}1\text{A}$ and $\text{WT}_w\text{-}3\text{A}$ are shown in Figure 4. The shape of the WAT is largely unaffected and its onset is reduced to only $1\text{ }^{\circ}\text{C}$, from $38\text{ }^{\circ}\text{C}$ for oil WT_w to $37\text{ }^{\circ}\text{C}$ for both oils $\text{WT}_w\text{-}1\text{A}$ and $\text{WT}_w\text{-}3\text{A}$. More notably, μ_{\max} of oil $\text{WT}_w\text{-}3\text{A}$ is three times that of oils WT_w and $\text{WT}_w\text{-}1\text{A}$, realized on cooling to $\sim 9\text{ }^{\circ}\text{C}$ (Table 4), despite only modest increases of 1–2% in aromatic and resin components on the addition of the asphaltic crude (Table 2). While the presence of asphaltenes has been shown to treat wax in a manner not unlike that of a PI in previous investigations [16,17], levels beyond this concentration do not prove beneficial in this oil. Although macroscopic phase separation is possible for higher concentrations [25], this phenomenon was not observed in our experiments. This is not surprising given that crudes with R/A ratios > 3 are typically stable (Table 2).

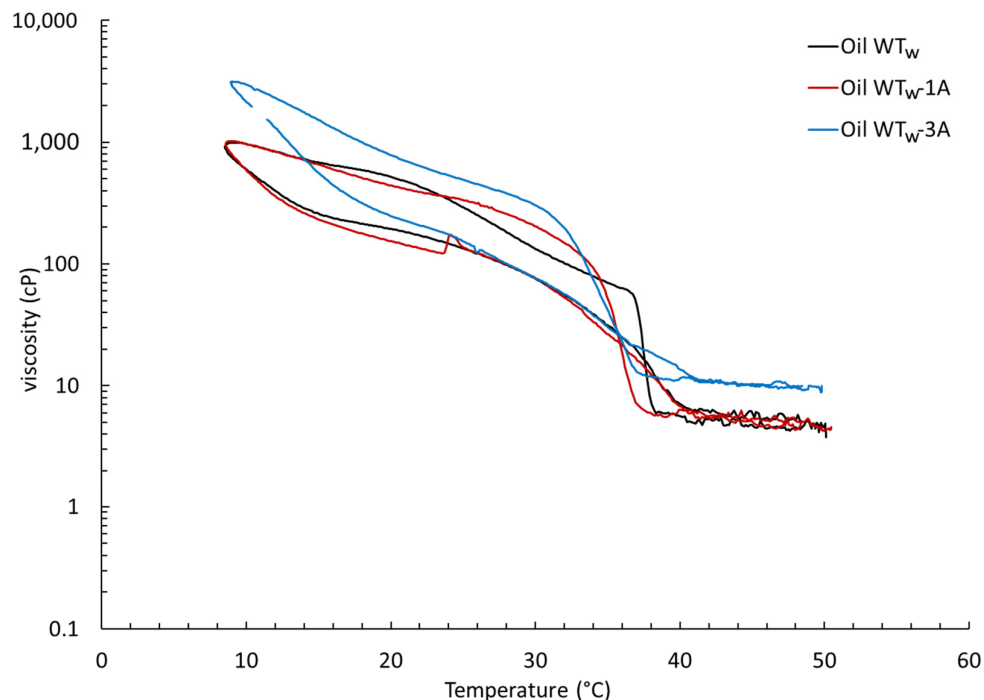


Figure 4. The $50\text{ }^{\circ}\text{C} \rightarrow 8\text{ }^{\circ}\text{C} \rightarrow 50\text{ }^{\circ}\text{C}$ cooling–heating viscosity profiles (cP) of oils WT_w (black), $\text{WT}_w\text{-1A}$ (red), and $\text{WT}_w\text{-3A}$ (blue).

3.3. Treatment of Wax and Asphaltenes

3.3.1. Wax in WT Crude, Treatment with ADs

Oil WT_w was treated separately with dispersants *AD3* and *AD4*, which performed best in heptane-induced instability tests. CPM images of the mixtures were collected 10 days after preparation for both treated and untreated oils WT_w , $\text{WT}_w\text{-AD3}$, and $\text{WT}_w\text{-AD4}$ (see Supporting Information Figure S4). Wax crystals can be observed in each of the three images, with little change in their consistency with perhaps fewer darker more amorphous deposits appearing in the image of oil $\text{WT}_w\text{-AD4}$ than the WT_w and $\text{WT}_w\text{-AD3}$. Little difference in either WAT or μ_{\max} was also observed (see Supporting Information Figure S5). Thus, from the point of view of either CPM or rheology, the dispersants do not notably alter the state of wax in the crude. This finding was not unexpected given that these additives, while having some structural similarities with PIs, differ in certain aspects such as accommodating asphaltenes.

3.3.2. Wax and Asphaltenes in WT Crude, Treatment with ADs

CPM images and $50\text{ }^{\circ}\text{C} \rightarrow 8\text{ }^{\circ}\text{C} \rightarrow 50\text{ }^{\circ}\text{C}$ cooling–heating viscosity profiles for oils $\text{WT}_w\text{-1A}$, $\text{WT}_w\text{-1A-AD3}$, and $\text{WT}_w\text{-1A-AD4}$ are given in Figures 5 and 6. Clusters of wax crystals appear more ordered and better solvated in the treated oils, particularly oil $\text{WT}_w\text{-1A-AD4}$. Darker more amorphous regions, which are likely asphaltene-rich, are better defined as well. However, treatment does little to alter WAT and μ_{\max} is increased by 37 and 60% on inclusion of the dispersants *AD3* and *AD4*, respectively (Table 4).

In previous studies involving the effect of treatment with PIs, we have shown that the degree of aggregation and particularly the interconnectivity of wax deposits in WT crude observed by CPM are strongly correlated with viscosity. The fact that this is not the case herein speaks to the difference in the structure of the PIs previously studied and the ADs being studied presently. While the PIs are based on AO-MA copolymers, the ADs are based on MA homopolymers. Perhaps more notable, however, is the method of attachment of pendant moieties to the backbones. Treatment of oil WT_w with a PI with amide/imide attachment functionality (Structure II) eventuated in a treated crude having significantly different rheological and morphological properties than crudes treated with PIs having

ester attachment functionality (Structure I) [17]. In some cases, the presence of clusters increases WAT and may serve as nucleation sites for wax crystal growth [27]. The fact that the wax crystals and asphaltene deposits observed in the CPM images appear less mingled, particularly in oil WT_w -1A-AD4, suggests that different mechanisms are at work in this system.

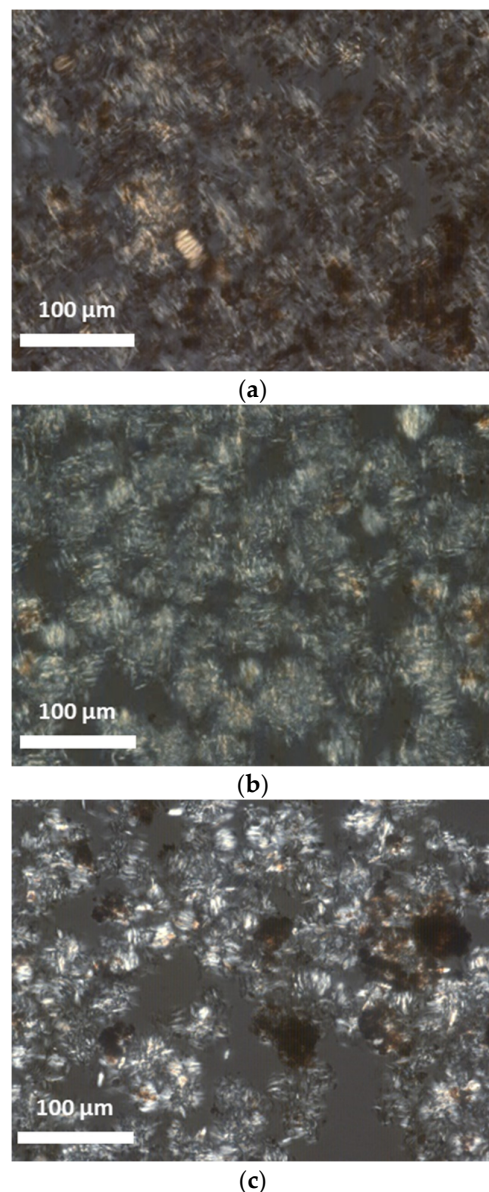


Figure 5. CPM images, taken following equilibration at 20 °C, of oils (a) WT_w -1A, (b) WT_w -1A-AD3, and (c) WT_w -1A-AD4.

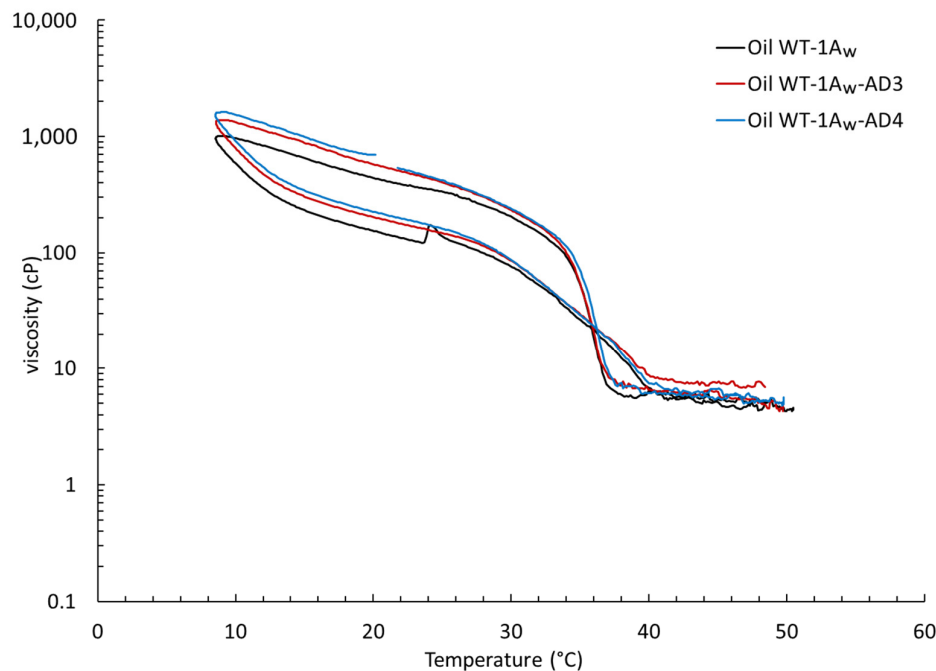


Figure 6. The $50\text{ }^{\circ}\text{C} \rightarrow 8\text{ }^{\circ}\text{C} \rightarrow 50\text{ }^{\circ}\text{C}$ cooling–heating viscosity profiles (cP) of oils $\text{WT}_w\text{-1A}$ (black), $\text{WT}_w\text{-1A-AD3}$ (red), and $\text{WT}_w\text{-1A-AD4}$ (blue).

3.3.3. Wax in WT Crude, Treatment with ADs and PI

Interactions between each of *AD3* and *AD4* with *PI* in *WT* crude were investigated by comparing oils WT_w , $\text{WT}_w\text{-PI}$, $\text{WT}_w\text{-AD3-PI}$, and $\text{WT}_w\text{-AD4-PI}$. CPM images of the oils appear in Figure 7. Treatment with *PI* effectively transforms the wax crystals from needle-like to more spherical discrete clusters. The addition of each of *AD3* and *AD4* eventuates in deposits with markedly different appearances. In both cases, the crystalline structures appear smaller than those in oil $\text{WT}_w\text{-PI}$ but these structures appear denser and less solvated in oil $\text{WT}_w\text{-AD3-PI}$ than in $\text{WT}_w\text{-AD4-PI}$.

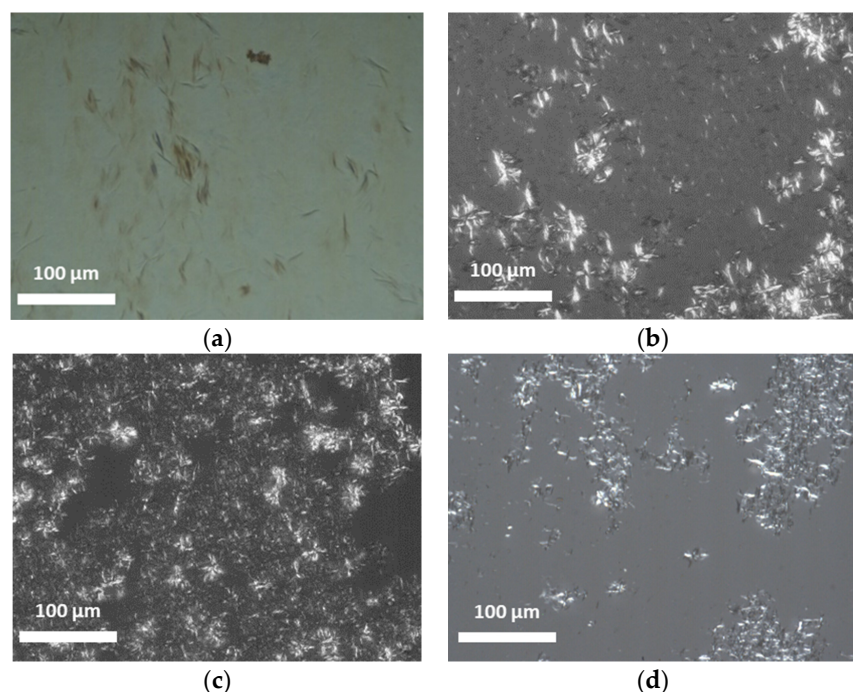


Figure 7. CPM images, taken following equilibration at $20\text{ }^{\circ}\text{C}$, of the oils (a) WT_w , (b) $\text{WT}_w\text{-PI}$, (c) $\text{WT}_w\text{-AD3-PI}$, and (d) $\text{WT}_w\text{-AD4-PI}$.

The viscosity cooling–heating profiles of oils WT_w , WT_w -PI, WT_w -AD3-PI, and WT_w -AD4-PI are shown in Figure 8. Treatment with PI reduces μ_{max} from 991 to 327 cP, a 67.0% reduction (Table 4), with the transformation in crystal morphology being consistent with this result. The addition of each of AD3 and AD4 increases μ_{max} to 367 and 595 cP, respectively. AD2-AD4 each contains 38–54 molar % of imidazoline-functional alkyl chains (AEAI) relative to all sidechains in the molecules. The additives also contain 46–62% of branched C20 (G20), branched C16 (G16), and linear C18 (TA) alkyl chains, respectively (Table 3). As such, these dispersants have been engineered to treat asphaltenes as well as wax and may more accurately be described as hybrid dispersants. Although AD3 and AD4 possess different fractions of AEAI, it is unlikely that this variation is responsible for differences in the viscosity profiles of the oils WT_w -AD3-PI and WT_w -AD4-PI because of the lack of such a correlation in heptane-induced stability tests. It is more likely that the lack of branching in the TA sidechains of AI3 relative to the G16 sidechains of AI4 is responsible for this difference.

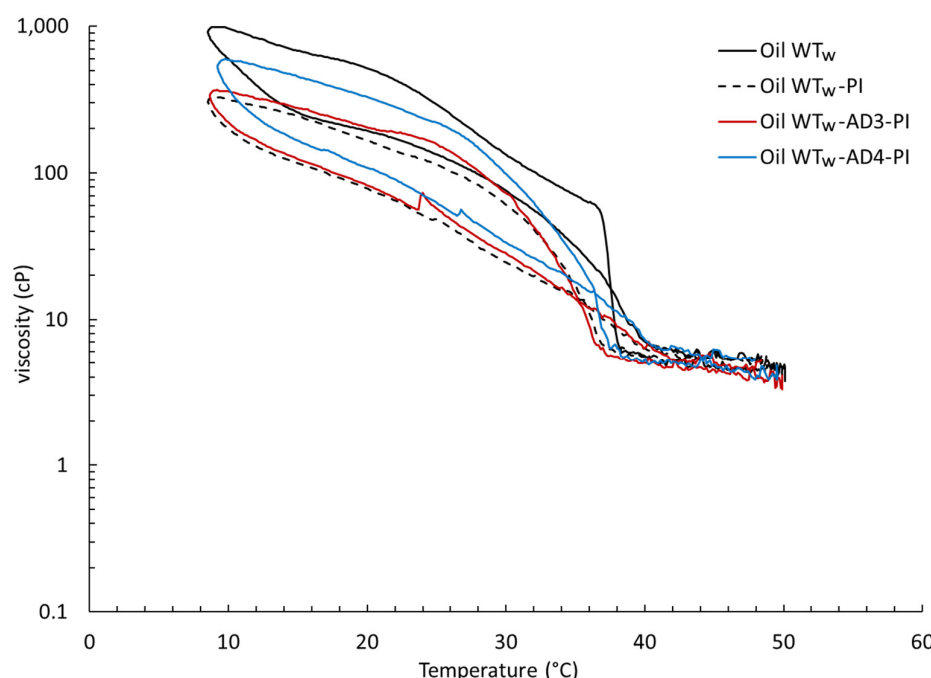


Figure 8. The $50\text{ }^{\circ}\text{C} \rightarrow 8\text{ }^{\circ}\text{C} \rightarrow 50\text{ }^{\circ}\text{C}$ cooling–heating viscosity profiles (cP) for oils WT_w -PI (black), WT_w -AD3-PI (red), and WT_w -AD4-PI (blue).

In past studies, we have found that wax-containing oils featuring more greatly solvated less inter-connected wax crystals generally have lower viscosities. The rheological data herein appear to be incongruent with CPM in that the wax crystals present in oil WT_w -AD3-PI, which features the lower viscosity profile of the two treated oils, appear to be less discrete, i.e., more inter-connected, than those in oil WT_w -AD4-PI, having the higher viscosity profile. As such, treatment with ADs has different rheological consequences than treatment with PI.

3.3.4. Wax and Asphaltenes in WT Crude, Treatment with ADs and PI

Treatment of crude containing both wax and asphaltenes by both ADs and PI was investigated in the oils WT_w -1A-PI, WT_w -1A-AD3-PI, and WT_w -1A-AD4-PI, with CPM images and $50\text{ }^{\circ}\text{C} \rightarrow 8\text{ }^{\circ}\text{C} \rightarrow 50\text{ }^{\circ}\text{C}$ cooling–heating viscosity profiles of these oils appearing in Figures 9 and 10. In all three oils, wax crystals and asphaltene clusters are clearly present, with little notable differences in morphology except perhaps that darker asphaltene clusters appear smaller and more dispersed in oil treated with AD3 than in oil treated with AD4. The viscosity profiles of oils WT_w -1A-PI and WT_w -1A-AD3-PI are nearly identical, having

no discernable WAT and μ_{\max} values of only 37 and 33 cP, a 96% reduction relative to oil WT_w. The viscosity profile of oil WT_w-1A-AD4-PI is only slightly higher, having a μ_{\max} of 133 cP, and likewise possesses no discernable WAT.

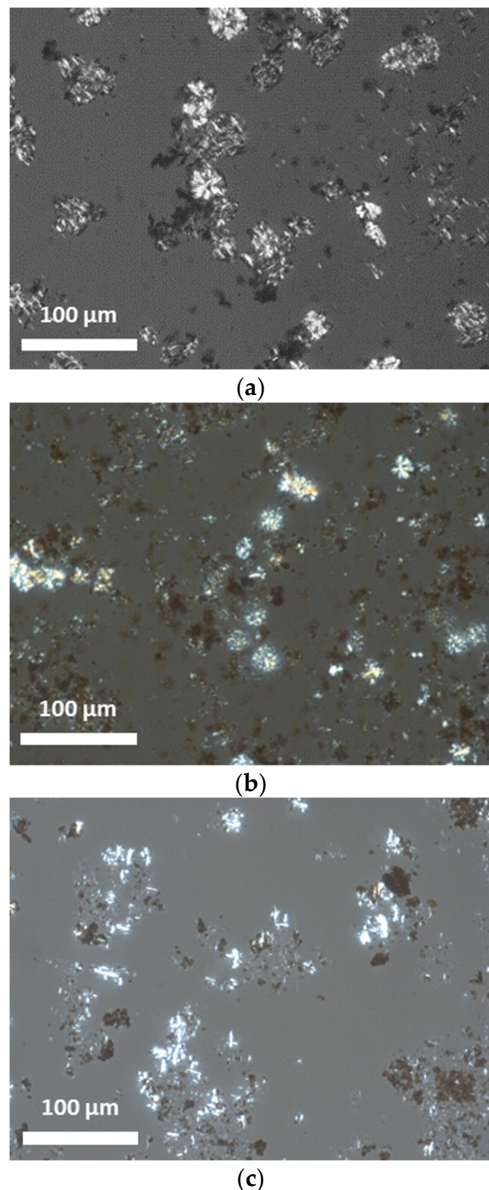


Figure 9. CPM images, taken following equilibration at 20 °C, of oils (a) WT_w-1A-PI, (b) WT_w-1A-AD3-PI, and (c) WT_w-1A-AD4-PI.

Wax is stabilized in crude by solvation shells consisting mainly of saturates of shorter chain lengths that remain liquid at the test temperature. Asphaltene clusters are stabilized by solvation shells consisting of both aromatic and resin components, the latter being composed of complex O-, N-, and S-functional molecules that are typically quite viscous or glass-like solids when isolated. The presence of these differing solvation shells, which do not typically appear under polarized light and therefore cannot be directly observed by this technique, affects rheology differently. Treatment of oils WT_w-1A, WT_w-PI, and WT_w-1A-PI, containing asphaltenes, PI, and both, with AD3, yields a lower profile than treatment with AD4.

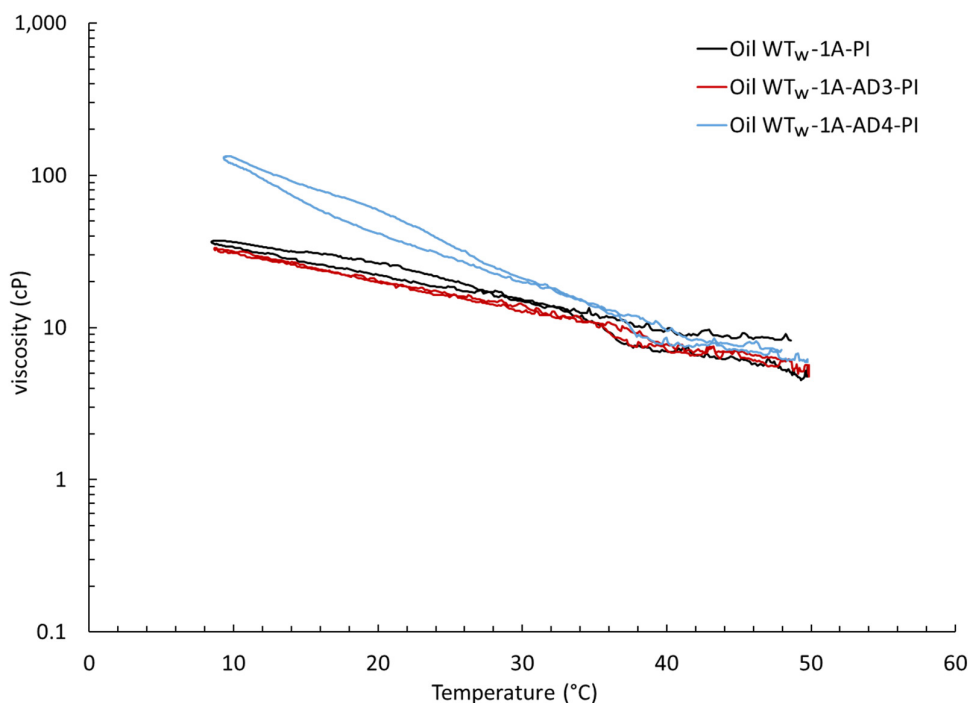


Figure 10. The $50\text{ }^{\circ}\text{C} \rightarrow 8\text{ }^{\circ}\text{C} \rightarrow 50\text{ }^{\circ}\text{C}$ cooling/heating viscosity profiles (cP) for oils $\text{WT}_w\text{-1A-PI}$ (black), $\text{WT}_w\text{-1A-AD3-PI}$ (red), and $\text{WT}_w\text{-1A-AD4-PI}$ (blue).

The AEAI-functional sidechains in *AD3* and *AD4* are basic whereas the asphaltic crude is acidic. Both ADs should therefore participate in favorable electrostatic interactions with asphaltenes and their resin precursors in the oils, with *AD4* having the potential to engage in a greater number of such interactions than *AD3*. In the same manner, the addition of toluene to dodecane likely reduces the number of favorable interactions between asphaltenes and wax, destabilizing the latter. Thus, enhanced interactions between asphaltenes and *AD4* relative to *AD3* may come at a similar expense. This reasoning may explain the reduction in the mingling of wax crystals and asphaltenes clusters seen in the CPM images, particularly in the absence of PI (i.e., the image of oil $\text{WT}_w\text{-1A-AD3}$ compared with that of oil $\text{WT}_w\text{-1A-AD4}$) and the rheological consequences of treatment on those oils. However, it is difficult to assess the degree to which the acidic and basic moieties are charged as the degree of protonation/deprotonation is likely to be attenuated in a water-deficient environment.

4. Summary and Conclusions

The introduction of low concentrations of asphaltenes into wax-containing oils can reduce viscosity but the effect is dependent on the concentration of aromatics in the oil. Viscosity increases with higher concentrations. Treatment of WT crude containing added wax with ADs does little to alter wax crystal morphology or rheology. However, treatment in the presence of asphaltenes results in fewer wax–asphaltene interactions, particularly treatment with *AD4*, the structural features of which render it more compatible with wax than those of *AD3*. The loss of these interactions eventuates in increases in the viscosity profiles of the oils despite the presence of larger solvation channels in the CPM images.

Treatment of added wax in WT crude with PI alone effectively transforms the continuous wax crystal network into discrete spherulites, lowering oil viscosity considerably. The addition of ADs to the treatment regimen appears to introduce more pronounced solvation channels between wax crystals, particularly in oil treated with *AD4*. However, further rheological benefits are not realized. Relative to the oil treated with PI alone, the inclusion of *AD3* has a minimal effect on viscosity while the inclusion of *AD4* increases viscosity. In the presence of asphaltenes, treatment with PI alone effects morphological changes that are similar to those observed in the absence of asphaltenes. However, the

viscosity of the treated oil is even lower than that of the analogous oil not containing added asphaltenes. The inclusion of ADs does not appear to affect wax crystal morphology appreciably, although asphaltene deposits appear to be somewhat better dispersed in the oils than in that treated with PI alone. The effects on oil viscosity mimic those in the absence of asphaltenes, with the inclusion of *AD3* having a minimal effect and the inclusion of *AD4* increasing viscosity relative to that of the oil treated with PI alone. While the structure of *AD4* more closely resembles that of the PI than *AD3*, *AD4* still possesses numerous AEAI sidechains, the presence of which likely renders the AD far less compatible with wax than the PI. If these structural similarities enhance interactions between *AD4* and the PI relative to those between *AD3* and the PI, then *AD4* could more effectively poison the function of the PI, resulting in the higher viscosities observed for oils treated with this AD. If true, these data illustrate the pitfalls of designing a flow assurance additive to interact with both wax and asphaltenes.

Trends have been identified regarding the morphological and rheological effects of treatment of wax-containing oils with ADs and PI in the presence and absence of asphaltenes. These include the effects of differences in the structural aspects of the ADs and compositions of the oils studied. However, incongruences in the degree of solvation of wax crystals and the degree of dispersion of asphaltenes with oil viscosity exist. Thus, our understanding of these interactions is incomplete. Recognizing that rheology is but one measure of the effectiveness of treatment and because the degree of wax deposition does not always correlate with viscosity [19], cold-finger deposition experiments combined with high-temperature gas chromatography (HTGC) analysis of deposited wax may provide a clearer picture. Electrical conductivity analysis to assess the effects of treatment on asphaltene particle size may yield further insights [39], with the ultimate goal of developing more effective flow assurance strategies.

Supplementary Materials: The following supporting information can be downloaded at: <https://www.mdpi.com/article/10.3390/colloids8030030/s1>, Figure S1. n-Alkane carbon number distribution of wax blend employed in experiments. Average carbon number equals 29.1 ± 3.8 . Figure S2. Refractive index vs. elution time gel permeation chromatograms of asphaltic crude (orange) and isolated asphaltenes in toluene (black) with peak and shoulder molecular weights, which represent nanoaggregates and clusters rather than individual molecules, noted. Figure S3. CPM images, taken following equilibration at 20°C , of oils (a) Dw and (b) Dw-1A. Figure S4. CPM images, taken following equilibration at 20°C , of oils (a) WTw, (b) WTw-AD3 and (c) WTw-AD4. Figure S5. $50^{\circ}\text{C} \rightarrow 8^{\circ}\text{C} \rightarrow 50^{\circ}\text{C}$ cooling-heating viscosity profiles (cP) of oils WT (black), WT-AD3 (red), and WT-AD4 (blue), each containing 10 wt. % wax.

Author Contributions: Conceptualization, O.M., J.C. and Q.P.N.; methodology, O.M., J.C. and Q.P.N.; validation, O.M. and Q.P.N.; formal analysis, O.M., J.C. and Q.P.N.; investigation, O.M. and Q.P.N.; resources, J.C. and Q.P.N.; data curation, O.M., J.C. and Q.P.N.; writing—original draft preparation, O.M.; writing—review and editing, O.M., J.C. and Q.P.N.; supervision, Q.P.N.; funding acquisition, Q.P.N. All authors have read and agreed to the published version of the manuscript.

Funding: This research was funded by Indorama Ventures Oxides and Derivatives LLC under the agreement UTA479562.

Data Availability Statement: Data are contained within the article.

Acknowledgments: The authors would like to thank Indorama Ventures Oxides and Derivatives LLC for their support in this work.

Conflicts of Interest: The authors declare no conflicts of interest. The funders had no role in the design of the study; in the collection, analyses, or interpretation of data; in the writing of the manuscript; or in the decision to publish the results. Author John Clements was employed by the company Indorama Ventures. The remaining authors declare that the research was conducted in the absence of any commercial or financial relationships that could be construed as a potential conflict of interest.

References

- Kelland, M.A. *Production Chemicals for the Oil and Gas Industry*, 2nd ed.; CRC Press: Boca Raton, FL, USA, 2014.
- Huang, Z.; Zheng, S.; Fogler, H.S. *Wax Deposition: Experimental Characterizations, Theoretical Modeling, and Field Practices*; CRC Press: Boca Raton, FL, USA, 2016.
- Bansal, R.; Ravishankar, B.; Sharma, S.S.; Afzal, K. Dynamic Simulation for Optimising Pigging Frequency for Dewaxing. In Proceedings of the SPE Oil and Gas India Conference and Exhibition, Mumbai, India, 28–30 March 2012.
- Buckley, J.S. Asphaltene Deposition. *Energy Fuels* **2012**, *26*, 4086–4090. [[CrossRef](#)]
- Leontaritis, K.J.; Ali Mansoori, G. Asphaltene deposition: A survey of field experiences and research approaches. *J. Pet. Sci. Eng.* **1988**, *1*, 229–239. [[CrossRef](#)]
- Vilas Bóas Fávero, C.; Hanpan, A.; Phichphimok, P.; Binabdullah, K.; Fogler, H.S. Mechanistic Investigation of Asphaltene Deposition. *Energy Fuels* **2016**, *30*, 8915–8921. [[CrossRef](#)]
- Soliman, F.S. *Paraffin: An Overview*; IntechOpen: London, UK, 2020.
- García, M.d.C. Crude Oil Wax Crystallization. The Effect of Heavy n-Paraffins and Flocculated Asphaltenes. *Energy Fuels* **2000**, *14*, 1043–1048. [[CrossRef](#)]
- García, M.C.; Carbognani, L.; Orea, M.; Urbina, A. The influence of alkane class-types on crude oil wax crystallization and inhibitors efficiency. *Pet. Sci. Eng.* **2000**, *25*, 99–105. [[CrossRef](#)]
- Wang, K.-S.; Wu, C.-H.; Creek, J.L.; Shuler, P.J.; Tang, Y. Evaluation of Effects of Selected Wax Inhibitors on Paraffin Deposition. *Pet. Sci. Technol.* **2003**, *21*, 369–379. [[CrossRef](#)]
- Borthakur, A.; Chanda, D.; Dutta Choudhury, S.R.; Rao, K.V.; Subrahmanyam, B. Alkyl Fumarate–Vinyl Acetate Copolymer as Flow Improver for High Waxy Indian Crude Oils. *Energy Fuels* **1996**, *10*, 844–848. [[CrossRef](#)]
- Al-Sabagh, A.M.; El-Hamouly, S.H.; Khidr, T.T.; El-Ghazawy, R.A.; Higazy, S.A. Preparation the Esters of Oleic Acid-Maleic Anhydride Copolymer and Their Evaluation as Flow Improvers for Waxy Crude Oil. *J. Dispers. Sci. Technol.* **2013**, *34*, 1585–1596. [[CrossRef](#)]
- Yang, F.; Zhao, Y.; Sjöblom, J.; Li, C.; Paso, K.G. Polymeric Wax Inhibitors and Pour Point Depressants for Waxy Crude Oils: A Critical Review. *J. Dispers. Sci. Technol.* **2014**, *36*, 213–225. [[CrossRef](#)]
- Atta, A.; Al-Shafy, H.; Ismail, E. Influence of ethylene acrylic alkyl ester copolymer wax dispersants on the rheological behavior of Egyptian crude oil. *J. Dispers. Sci. Technol.* **2011**, *32*, 1296–1305. [[CrossRef](#)]
- Fang, L.; Zhang, X.; Ma, J.; Zhang, B. Investigation into a pour point depressant for Shengli crude oil. *Ind. Eng. Chem. Res.* **2012**, *51*, 11605–11612. [[CrossRef](#)]
- M'barki, O.; Clements, J.; Salazar, L.; Machac, J.; Nguyen, Q.P. Effects of Structure and Asphaltenes on Paraffin Inhibitor Efficacy in a Light Crude Oil Model. *Energy Fuels* **2022**, *36*, 7531–7541. [[CrossRef](#)]
- M'barki, O.; Clements, J.; Salazar, L.; Machac, J.; Nguyen, Q.P. Effects of oil composition on interactions between paraffinic and asphaltene components and the performance of paraffin inhibitors. *Geoenergy Sci. Eng.* **2023**, *225*, 211699. [[CrossRef](#)]
- M'barki, O.; Clements, J.; Salazar, L.; Machac, J.; Nguyen, Q.P. Impact of Paraffin Composition on the Interactions between Waxes, Asphaltenes, and Paraffin Inhibitors in a Light Crude Oil. *Colloids Interfaces* **2023**, *7*, 13. [[CrossRef](#)]
- M'barki, O.; Clements, J.; Nguyen, Q.P. Effects of Added Asphaltenes and Paraffin Inhibitor on Wax Stability and Deposition in Oils of Varying Complexity. *Energy Fuels* **2023**, *37*, 14790–14799. [[CrossRef](#)]
- Yen, A.; Yin, Y.R.; Asomaning, S. Evaluating asphaltene inhibitors: Laboratory tests and field studies. In Proceedings of the SPE International Symposium on Oilfield Chemistry, Houston, TX, USA, 13–16 February 2001; OnePetro: Richardson, TX, USA, 2001.
- Juyal, P.; Enayat, S.; Luente-Schultz, R.; Li, Q.; Karimipour, M.; Tavakkoli, M.; Cao, T.-B.; Yen, A.; Russell, C.; Vargas, F.M. Case Study: Investigation of the Performance of an Asphaltene Inhibitor in the Laboratory and the Field. *Energy Fuels* **2022**, *36*, 1825–1831. [[CrossRef](#)]
- Ovalles, C.; Rogel, E.; Morazan, H.; Moir, M.E. Synthesis, characterization, and mechanism of asphaltene inhibition of phospho-propoxylated asphaltenes. *Fuel* **2016**, *180*, 20–26. [[CrossRef](#)]
- Ilyin, S.; Arinina, M.; Polyakova, M.; Bondarenko, G.; Konstantinov, I.; Kulichikhin, V.; Malkin, A. Asphaltenes in heavy crude oil: Designation, precipitation, solutions, and effects on viscosity. *J. Pet. Sci. Eng.* **2016**, *147*, 211–217. [[CrossRef](#)]
- Li, C.; Zhu, H.; Yang, F.; Liu, H.; Wang, F.; Sun, G.; Yao, B. Effect of Asphaltene Polarity on Wax Precipitation and Deposition Characteristics of Waxy Oils. *Energy Fuels* **2019**, *33*, 7225–7233. [[CrossRef](#)]
- Venkatesan, R.; Östlund, J.-A.; Chawla, H.; Wattana, P.; Nydén, M.; Fogler, H.S. The Effect of Asphaltenes on the Gelation of Waxy Oils. *Energy Fuels* **2003**, *17*, 1630–1640. [[CrossRef](#)]
- Kriz, P.; Andersen, S.I. Effect of asphaltenes on crude oil wax crystallization. *Energy Fuels* **2005**, *19*, 948–953. [[CrossRef](#)]
- Tinsley, J.F.; Jahnke, J.P.; Dettman, H.D.; Prud'home, R.K. Waxy gels with asphaltenes 1: Characterization of precipitation, gelation, yield stress, and morphology. *Energy Fuels* **2009**, *23*, 2056–2064. [[CrossRef](#)]
- Ariza-León, E.; Molina-Velasco, D.-R.; Chaves-Guerrero, A. Review of studies on asphaltene-wax interaction and the effect thereof on crystallization. *CTF-Cienc. Tecnol. Y Futuro* **2014**, *5*, 39–53. [[CrossRef](#)]
- Yang, F.; Zhu, H.; Li, C.; Yao, B.; Wang, F.; Chen, J.; Sun, G. Investigation on the mechanism of wax deposition inhibition induced by asphaltenes and wax inhibitors. *J. Pet. Sci. Eng.* **2021**, *204*, 108723. [[CrossRef](#)]
- Barre, L.; Eyssautier, J.; Mullins, O.; Barre, L.; Eyssautier, J.; Mullins, O. The asphaltenes. *Annu. Rev. Anal. Chem.* **2011**, *4*, 393–418.

31. Mullins, O.C.; Sabbah, H.; Eyssautier, J.; Pomerantz, A.E.; Barré, L.; Andrews, A.B.; Ruiz-Morales, Y.; Mostowfi, F.; McFarlane, R.; Goual, L.; et al. Advances in asphaltene science and the Yen–Mullins model. *Energy Fuels* **2012**, *26*, 3986–4003. [[CrossRef](#)]
32. Mullins, O.C. The Modified Yen Model. *Energy Fuels* **2010**, *24*, 2179–2207. [[CrossRef](#)]
33. Kok, M.V.; Saracoglu, R.O. Mathematical modelling of wax deposition in crude oil pipelines (comparative study). *Pet. Sci. Technol.* **2000**, *18*, 1121–1145. [[CrossRef](#)]
34. Xiong, R.; Guo, J.; Kiyingi, W.; Feng, H.; Sun, T.; Yang, X.; Li, Q. Method for Judging the Stability of Asphaltenes in Crude Oil. *ACS Omega* **2020**, *5*, 21420–21427. [[CrossRef](#)]
35. Moncayo-Riascos, I.; Taborda, E.; Hoyos, B.A.; Franco, C.A.; Cortés, F.B. Effect of resin/asphaltene ratio on the rheological behavior of asphaltene solutions in a de-asphalting oil and p-xylene: A theoretical–experimental approach. *J. Mol. Liq.* **2020**, *315*, 113754. [[CrossRef](#)]
36. Asomaning, S.; Watkinson, P. Petroleum Stability and Heteroatom Species Effects in Fouling of Heat Exchangers by Asphaltenes. *Heat Transf. Eng.* **2000**, *21*, 10–16.
37. Ashoori, S.; Sharifi, M.; Masoumi, M.; Mohammad Salehi, M. The relationship between SARA fractions and crude oil stability. *Egypt. J. Pet.* **2017**, *26*, 209–213. [[CrossRef](#)]
38. Sinnathamb, C.M.; Nor, N.M. Relationship between SARA fractions and crude oil fouling. *J. Appl. Sci.* **2012**, *12*, 2479–2483. [[CrossRef](#)]
39. Yang, F.; Li, C.; Yang, S.; Zhang, Q.; Xu, J. Effect of dodecyl benzene sulfonic acid (DBSA) and lauric amine (LA) on the associating state and rheology of heavy oils. *J. Pet. Sci. Eng.* **2014**, *124*, 19–26. [[CrossRef](#)]

Disclaimer/Publisher’s Note: The statements, opinions and data contained in all publications are solely those of the individual author(s) and contributor(s) and not of MDPI and/or the editor(s). MDPI and/or the editor(s) disclaim responsibility for any injury to people or property resulting from any ideas, methods, instructions or products referred to in the content.